Medical Devices and Diagnostic Engineering

Research Article ISSN: 2399-6854

Assessment of a novel supercritical nitrogen cryosurgical device using prostate and renal cancer tissue engineered models

Anthony T Robilitto[1], Kimberly L Santucci[1], Kristi K Snyder[1], Robert G Van Buskirk[1-3], John G Baust[1-3] and John M Baust[1*]

[1]CPSI Biotech, 2 Court St., Owego, NY 13827, USA

[2]Center for Translational Stem Cell and Tissue Engineering Binghamton University, 4400 Vestal Parkway East, Binghamton, NY 13902, USA

[3]Department of Biological Sciences, Binghamton University, 4400 Vestal Parkway East, Binghamton, NY 13902, USA

Abstract

Objective: Growing adoption of cryoablation to treat cancer is driving a need for a deeper understanding of the dynamics of the freezing process at the engineering and biological level. We previously reported on a tissue engineered model (TEM) that provides a freeze medium with clinically relevant volumes and thermal characteristics, while allowing for the post-thaw assessment of cellular ablation. In this study, we utilized TEMs to assess the performance of the supercritical nitrogen (SCN) cryosurgical device.

Methods: Assessment included freeze zone isotherm characterization and ablation in heat loaded TEMs. Two cryoprobes (2.0 mm x 4.0 cm and a 1.8 mm x 3.0 m freeze zone SCN cryoprobe) and a 5/5/5 min freeze/thaw/freeze procedure was performed on prostate (pTEM) or renal cancer (rTEM) models.

Results: Analysis revealed the 1.8 mm cryoprobe (pTEM) generated 28.87 cm^3 iceball and the 2.0 mm cryoprobe (rTEM) generated 33.33 cm^3 iceball. The -20°C and -40°C isotherms penetrated 2.53 cm (±0.11) and 2.02 cm (±0.1) from the probe surface in pTEMs and 2.65 cm (± 0.13) and 2.10 cm (± 0.09) in rTEMs, comprising 45.3% and 28.7% of the frozen volumes in both models. Analysis of ablative capacity at 1 and 24 hours revealed 60.4% (pTEM) and 78.9% (rTEM) of the frozen volume was destroyed. Comparison of live/dead imaging with thermal profiles suggested a critical lethal temperature of -30°C for prostate cancer and -20°C for renal cancer TEMs corresponding with previous reports.

Conclusions: The findings demonstrate that the SCN cryosurgical system was able to generate large ablative volumes under physiological heat loads more rapidly than current technologies. This is important as it is well appreciated in clinical practice that the heat load of a tissue, cryoprobe proximity to vasculature, etc. can impact outcome. Overall, these studies suggest that SCN Cryosystem allows for the rapid and controlled application of ultra-cold temperatures and efficient freezing of targeted tissue.

Introduction

Cryoablative therapies rely on the precise placement of a cryoprobe and the circulation of a cryogen within the probe to extract thermal energy to achieve freezing temperatures within the targeted tissue [1-3]. The growth in the use of cryoablative therapies has been driven by several factors. Technological advancements such as planning software and intraoperative ultrasound that guide cryoprobe placement and track the advancing ice front, fine gauge thermocouple needles that accurately monitor tissue temperatures, devices that can warm and protect adjacent, non-targeted tissues and multi-probe cryosurgical devices able to sculpt the cryolesion, have made cryoablative therapies more consistent and effective [4,5]. In addition to technological improvements, a growing understanding of the molecular responses of the cells and tissues to freezing insults has made the field more translational and evidence based [6-10]. which is consistent with publications of long term follow-up studies showing comparative results between cryoablation and traditional procedures [11-17]. Additionally, a best practice guideline published by the American Urological Association (AUA) on prostate cryosurgery has provided standardization for clinical applications [18]. Despite these advancements, however, several issues affecting the successful application of cryotherapies persist. Chief among these is management of the freeze zone periphery [19-21].

During a cryosurgical procedure, the circulating cryogen within the cryoprobe extracts heat energy from the surrounding tissue and, as temperatures drop, ice begins to form. As heat is removed, thermal gradients are generated in which the distance from the cryoprobe surface impacts cooling rate and nadir temperature experienced by the tissue. As the distance from the cryoprobe increases, cooling rates decrease, and temperatures increase. Under intraoperative ultrasound, the outer edge of the ice front appears hyperechoic and is readily observable as it grows outward from the cryoprobe surface [22]. Yet, the extent of cell death is located some distance behind this hyperechoic rim, and is determined by a number of factors including the tissue or cell type (sensitivity) being targeted, the cooling rate, the nadir temperature produced in the tissue, the duration of tissue exposure to

Correspondence to: John M. Baust, CPSI Biotech 2 Court St. Owego, NY 13827, USA, Tel: 607 687-8701; E-mail: jmbaust@cpsibiotech.com

Key words: *thermal ablation, cryosurgery, tissue engineered model, supercritical nitrogen, SCN system, cell death, prostate cancer, renal cancer*

Received: December 03, 2019; **Accepted:** December 17, 2019; **Published:** December 23, 2019

cryogenic temperatures, the thawing rate, and the number of freeze/thaw cycles [5,8,9,20,23]. Within the periphery of the freeze zone, between the lethal isotherm, defined as the temperature below which cell death is assured, and the edge of the iceball, lies a volume of partial tissue destruction. Clinically, it is important to minimize the amount of targeted tissue that lies within this zone, as it increases the risk for disease recurrence [24,25]. Management of the freeze zone periphery, therefore, is of critical importance to cryoablative efficacy.

To ensure that the entire volume of the targeted tissue is destroyed, a positive freeze margin (typically 0.5 - 1 cm) is often created, when possible, in which the freeze zone is extended beyond the outer edge of the targeted volume [18,19,23]. This is done to increase the probability that the targeted tissue achieves temperatures at, or below, the critical lethal isotherm (between -20°C and -40°C, cancer dependent) [24,26]. Given the geometry of the freeze zone, however, with today's commercial cryodevices the volume of this positive freeze margin can often equal or exceed the volume of the targeted tissue, resulting in the partial destruction of a non-targeted tissue [24,27]. Alternatively, when a positive freeze margin is not employed a substantial volume of targeted tissue may not be fully eradicated. Efforts to reduce the non-targeted death associated with the positive freeze margin while reducing the chance of partial lethality in targeted tissue, have focused on the development of adjunctive agents and combinatorial treatment modalities to sensitize cells to freezing insults [10,24,28-31]. This strategy is designed to raise the minimal lethal temperature thereby reducing the need for a positive freeze margin and the chance of cancer survival within the periphery of the frozen mass. Another method to reduce the extent of the freeze margin and improve cryotherapeutic efficacy is by employing a colder, more efficient cryogen to drive lethal temperatures deeper in to target tissue [5,32].

Current cryosurgical devices can be characterized by the type of cryogen employed [5]. The most common, and current industry standard, cryodevices utilize a compressed gas (typically argon or nitrous oxide) undergoing Joule-Thomson (JT) cooling. These JT devices can use small diameter probes that generate freezing temperatures near instantaneously (<5 sec), but due to the gaseous cryogen's low thermal conductivity (e.g. work capacity), JT devices often require large numbers of probes and/or extended freeze times. In contrast, cryosurgical devices employing liquid nitrogen (LN_2) offer superior heat extraction, but due to the boiling and subsequent phase change of the liquid into gas, LN_2 cryoprobes are typically larger and slower acting. Additionally, larger probes and umbilical's retain a bolus of liquid cryogen after probe "inactivation" that may result in extended freezing after user-controlled probe inactivation.

In an attempt to achieve the speed and miniaturization of JT systems, yet maintain the cooling capacity of liquid systems, we developed a novel cryosurgical platform utilizing supercritical nitrogen (SCN) as the cryogen [33]. We have previously reported on the use of the SCN Cryosystem for the targeted delivery of ablative temperatures in cardiac tissue [34,35]. These studies revealed that SCN provides for a significant improvement in performance compared to other cardiac cryosystems. In this study we investigated the potential for the use of the SCN Cryosystem for the ablation of solid cancerous tumors. To this end, we examined the ablative capacity of the SCN cryosystem using a 3-dimensional (3D) tissue engineered prostate and renal cancer model (TEM) [27,36,37]. By using the TEMs in conjunction with thermocouple arrays and live/dead fluorescent imaging, we were able to assess the size, thermal profile, and lethality of the freeze zone generated by the SCN cryosurgical system.

Methods

Cell and 3D cultures

The human prostate (PC-3) and renal (786-O) cancer cell lines were obtained from the ATCC (Rockville, MD). Cultures were maintained at 37°C, 5% CO_2: 95% air in RPMI-1640 culture medium (Caisson Laboratories Inc., Logan City, UT) fortified with 10% FBS (Atlanta Biologics Inc., Atlanta, GA) and 1% penicillin/streptomycin (Corning, Inc. Corning NY). Cells were cultured in 75 cm^2 t-flasks with media replenishment every three days.

For generation of the tissue engineered models (TEM), rat tail type I collagen solution (BD Bioscience, Bedford, MA) was used to form 0.2% w/v gel matrices as per SOP. Cells, Prostate: 0.85-1.2 x 10^6 cells/mL and Renal 0.65-0.8 x 10^6 cells/mL, were suspended in the collagen solution prior to solidification in 3 mm x 60 mm TEM ring fixtures as per Robilotto *et al.* and Baust *et al.* [27,32,36-38]. The TEM cell containing matrices were cultured for 24 hours prior to utilization. All experiments were performed between cell passages 5 and 20.

Freezing protocol

Prior to freezing, individual cell seeded TEMs were assembled into the 3-D stack configuration (60 mm x 60 mm) following SOP [27,36,38] (Figure 1). The TEM stack was then submerged into a warm circulating bath of culture media followed by placement onto a heat pad and stir table and a cryoprobe and thermocouple array were then inserted to monitor temperatures (Figure 1). Samples were held until TEM and bath temperatures equilibrated at 32° C (±2°C), TEM samples were frozen using the SCN Cryosystem using a 1.8 mm or 2.0 mm diameter SCN cryoprobe with a 1.8 mm x 3 cm (prostate) or 2.0 mm x 4 cm (renal) freeze zone at the distal tip. TEM models were frozen using a 5/5/5 (in minutes) freeze/thaw/freeze protocol. Temperature of the bath and within the TEM were monitored throughout the freezing process

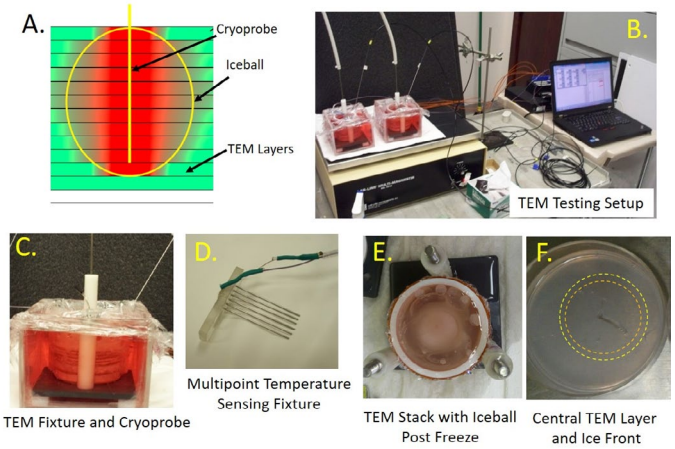

Figure 1. Illustration of TEM and the freezing apparatus setup

TEM models were assembled into 3-D stacks and placed into a bath of warm media on a warming pad and a stir table to facilitate media circulation during freezing. Cryoprobe were placed into the center of the TEM with the cryoprobe freeze zone centered vertically within the TEM. Temperatures of the TEM and bath were monitored throughout the freeze protocol. A) Schematic of a TEM stack with cryoprobe inserted and iceball, B) Image of a testing freeze setup including TEMs, cryoprobe, heat source, stir table, TempScan and PC monitoring station , C) Close up of the TEM apparatus with probe and thermocouple array inserted D) Photo of the thermocouple array used to monitor temperature distribution radiating from the center point of the cryoprobe ablation segment, E) Photo of a frozen TEM stack (note opaque iceball in center of TEM) and F) Photo of the TEM layer from the freeze zone center illustrating the visible iceball edge following the first (orange ring) and second freeze (yellow ring)

at fixed distances of 7.5 mm 10.5 mm, 13 mm, 16 mm, and 19 mm extending radially from the surface of the cryoprobe at the center point of the freeze zone (i.e. 1.5 cm for prostate and 2 cm for renal studies) using a type-T multipoint thermocouple array (Figure 1) and recorded with an Omega TempScan at 10 sec intervals throughout the entire freeze cycle. At the completion of the freeze cycle, TEMs were allowed to passively thaw in the warm circulating bath for 30 minutes prior to disassembly at which time the individual TEM layers were returned to culture for recovery and assessment [21,32]. (Figure 1).

TEM assessment

Following thawing and disassembly, individual TEM layers were measured via calipers to determine the diameter of the iceball created following the 1st and 2nd freezes of the freeze-thaw cycle (Figure 1). Iceball radii were also measured at cardinal locations around the probe surface to determine symmetry of the freeze zone created. Individual layers were then bisected at the probe center yielding two replicate samples from each layer for analysis. One half of the layer sample was then placed into culture to assess 24 Hr post-freezing recovery while the other half was assessed for immediate (1 Hr) post-freeze viability. *In situ* sample viability assessment was performed using the fluorescent probes Calcein AM and Propidium Iodide (Cal/PI; Invitrogen). Briefly, culture medium was decanted from the TEM samples and 2 mL of the working Cal/PI solution (10 ul Cal + 8 ul PI + 2 ml PBS) was added directly to each sample. Samples were incubated in the dark at 37°C for 60 min (±1 min). Fluorescent staining was visualized using a Zeiss Axiovert 200 fluorescent microscope under a 10X magnification with the AxioVision 4 software (Carl Zeiss, Germany). Panoramic digital images were recorded starting at the iceball center (probe surface) and extended across the freeze region into the non-frozen periphery. Following acquisition, a 5000 μm (5 mm) scale bar and reference mark at a radius of 15 mm (representing a 3 cm diameter) was auto-imprinted onto each of the images using the AxioVision software to enable direct image comparison.

Data analysis

For iceball and thermal profile assessment, a minimum of 7 repeats per probe were conducted. For ablation zone imaging studies, a minimum of three TEM repeats per cancer type (prostate and renal) were conducted. Following experimentation, data were combined and averaged (±SD) to determine mean iceball size, temperature location and ablation zone produced. Iceball, thermal zone and ablation volumes were calculated based on freeze zone center point TEM layer measurements using an ellipsoid model to enable volumetric analysis of system performance.

Freeze zone size: Following the freeze/thaw episode, iceball diameter and radii were measured using digital calipers at the center point of the cryoprobe freeze zone.

Ablation zone: Fluorescent imaging of the TEM at the center point of the cryoprobe, images were measured using the AxioVision software to determine the size of the zone of ablation (PI positive/ Calcein negative (red) region).

Thermal profiles: Real time recordings of the thermal profiles collected using the Omega TempScan system were converted to graphical format using Microsoft Excel and analyzed to determine isotherm spread during the 1st and 2nd freeze intervals.

Results

SCN cryosystem performance studies

To assess the performance of the SCN Cryosystem, a series of freeze studies were conducted utilizing prostate (pTEM) and renal (rTEM) tumor models. For the pTEM, experiments were performed using a 1.8 mm SCN cryoprobe (1.8 mm x 3 cm freeze zone) for analysis of freezing and prostate cancer cell destruction. For the rTEM, experiments were performed using a 2.0 mm SCN cryoprobe (2.0 mm x 4 cm freeze zone). The 3 cm and 4 cm freeze zone lengths were selected as these lengths are utilized in current commercial cryoprobes for prostate and renal tumor ablation, respectively [27,32,39].

Iceball analysis and comparison

To assess overall iceball size following a 5/5/5 freeze protocol, pTEM (prostate cancer) samples were frozen, allowed to thaw, disassembled into individual layers and the layer at the center of the freeze zone (1.5 cm) was measured to determine the size (diameter) of the frozen mass following the first and second freeze episode. This assessment is possible following thawing as each ice front leaves a distinct visible ring where the edge of the iceball [27,32] (Figure 1). These rings represented the transition from frozen to non-frozen TEM tissue and have been previously reported to correlate to a temperature of ~-2°C [18,19,22,27]. Assessment of iceball diameter following pTEM freezing using the 1.8 mm x 3.0 cm SCN cryoprobe revealed an average diameter of 3.00 cm (±0.1 cm) following the 1st freeze and 3.86 cm (±0.17 cm) following the 2nd freeze (Table 1). Volumetric analysis of the iceball formed by the 1.8 mm SCN cryoprobe revealed a 17.44 cm^3 frozen mass following the 1st freeze and a 28.87 cm^3 frozen mass following the 2nd freeze.

For assessment of overall iceball size created using the 2.0 mm SCN cryoprobe with a 4 cm freeze zone length (2.0 mm x 4.0 cm), renal cancer rTEM samples were frozen under the 5/5/5 protocol. As with pTEMs, the rTEM layer at the center of the freeze length was measured to determine the size (diameter) of the frozen mass following the first and second freeze. Assessment of iceball diameter following rTEM freezing revealed the formation of an iceball with an average diameter of 3.10 cm (±0.13 cm) following the 1st freeze and 3.94 cm (±0.19 cm) following the 2nd freeze (Table 1). Volumetric analysis of the iceball formed by the 2.0 mm SCN cryoprobe revealed a 20.63 cm^3 frozen volume following the 1st freeze and a 33.33 cm^3 frozen volume following the 2nd freeze. The formation of a larger iceball created by the SCN cryoprobe in the rTEM compared to the pTEM was expected given the 28% increase in freeze zone surface area in the 2.0 mm x 4.0 cm cryoprobe compared to the 1.8 mm x 3.0 cm freeze zone, which translated to a ~15% increase in the overall frozen volume in the rTEMs (33.33 cm^3 vs. 28.87 cm^3, respectively).

pTEM isotherm analysis and comparison

Iceball size is often utilized as a comparative metric for the performance of cryosurgical devices, however iceball size does not reflect isotherm distribution within the frozen mass [3,5,20,27,39]. Given this, assessment of isothermal distribution was assessed within

Table 1. Average measurements of the iceball created by a SUN cryoprobe in the TEM model following a 5/5/5 freeze

	Average Lethal Isotherm Diameter (cm(±SD))		Iceball Volume (cm)	Iceball Volume (cm)
	1st Freeze	2nd Freeze	1st Freeze (cm^3)	2nd Freeze (cm^3)
pTEM (1.8mm)	3.00 (±0.1)	3.86 (±0.17)	17.44	28.87
rTEM (2.0rnm)	3.10 (±0.13)	3.96 (±0.19)	20.63	33.33

the TEMs during freezing using the SCN Cryosystem. Thermal profile assessment was conducted at 5 fixed positions extending from the probe surface at the center of the probe freeze zone (Figure 2). Isotherm assessment studies using the 1.8 mm x 3.0 cm SCN cryoprobe following the 5/5/5 protocol revealed an isothermal profile characterized by the -20°C isotherm at a diameter of 2.18 cm (±0.09 cm) and 2.53 cm (±0.11 cm) following the 1st and 2nd 5min freeze, respectively (Table 2). Examination of the -40°C isotherm revealed a 1.75 cm (±0.05 cm) and 2.02 cm (±0.01 cm) diameter following the 1st and 2nd freeze, respectively. Volumetrically, this correlated to 13.41 cm^3 and 8.55 cm^3 of the 28.87 cm^3 frozen mass being at or below -20° and -40°C, respectively. Comparing the penetration of the lethal isotherm to that of the overall frozen mass created by the SCN cryoprobe, it was found that 46.4% and 29.6% of the total volume of the frozen pTEM was ≤-20°C and -40°C, respectively.

As in the pTEM studies, assessment of the isothermal profile following the initial 5 mins of freezing of the rTEM using the 2.0 cm x 4.0 cm SCN cryoprobe revealed a lethal -20°C isotherm diameter of 2.29 cm (±0.11 cm) and the -40°C isotherm diameter of 1.8 cm (±0.05 cm) (Table 2). After completion of the 2nd 5 min freeze, the -20°C and -40°C isotherm diameters were found to extend to 2.65 cm (±0.13 cm) and 2.1 cm (±0.09 cm), respectively. Volume equaled 14.71 cm^3 and 9.24 cm^3 out of the total 33.33 cm^3 frozen mass being at or below -20° and -40°C, respectively. In relation to the overall frozen volume following the 5/5/5 protocol, 44.1% of the iceball was at -20°C or below and 27.7% at or below -40°C.

TEM ablation analysis

In addition to the size and isotherm distribution of the freeze zone generated with the SCN system within the pTEM model for the 1.8 mm x 3.0 cm SCN cryoprobe, image analysis utilizing the live/dead assay and fluorescent microscopy was conducted to evaluate the overall ablative impact on the constituent prostate cancer cells within the TEM. For evaluation of the level of cellular destruction, examination of the TEM layer at the center of the probe freeze zone (1.5 or 2.0 cm) was conducted following completion of the 5/5/5 double freeze procedure. Fluorescent imaging of TEM layers probed with calcein AM (green, live) and propidium iodide (red, dead) at 1 hr and 24 hr post-thaw was conducted to determine the immediate and delayed ablative effects of the 5/5/5 min freeze procedure. The 1 and 24 hour time points were selected to allow for assessment of immediate cell death as well as for identification of any delayed cell responses (death or recovery) within the TEM, such as in the periphery where sub-lethal freezing temperatures are achieved (i.e. warmer than -30°C for prostate cancer) [2-4,7,37].

Analysis of prostate cancer cell destruction following freezing with the 1.8 mm x 3.0 cm SCN cryoprobe revealed near complete destruction extending to 1.45 cm (±0.1 cm) from the probe surface yielding a 2.89 cm (±0.3 cm) diameter lethal zone around the SCN cryoprobe at the center of the freeze zone (Figure 3). Correlating the zone of destruction with the isotherm profile data revealed a transition from cell destruction to survival occurring around the -30°C isotherm with the SCN system which matches published results of *in vitro* studies [19,20,26]. This resulted in a 0.49 cm (±0.1 cm) rim of incomplete cell destruction within the perimeter of the pTEM frozen mass. Follow-up analysis at 24 hours post freeze revealed minimal recovery prostate cancer cells within the periphery of the iceball when compared to the 1 hour post freeze (Figure 3). Volumetrically, the ablative zone generated in the pTEM averaged 17.43 cm^3, calculating to 60.4% of the total frozen volume (Table 3).

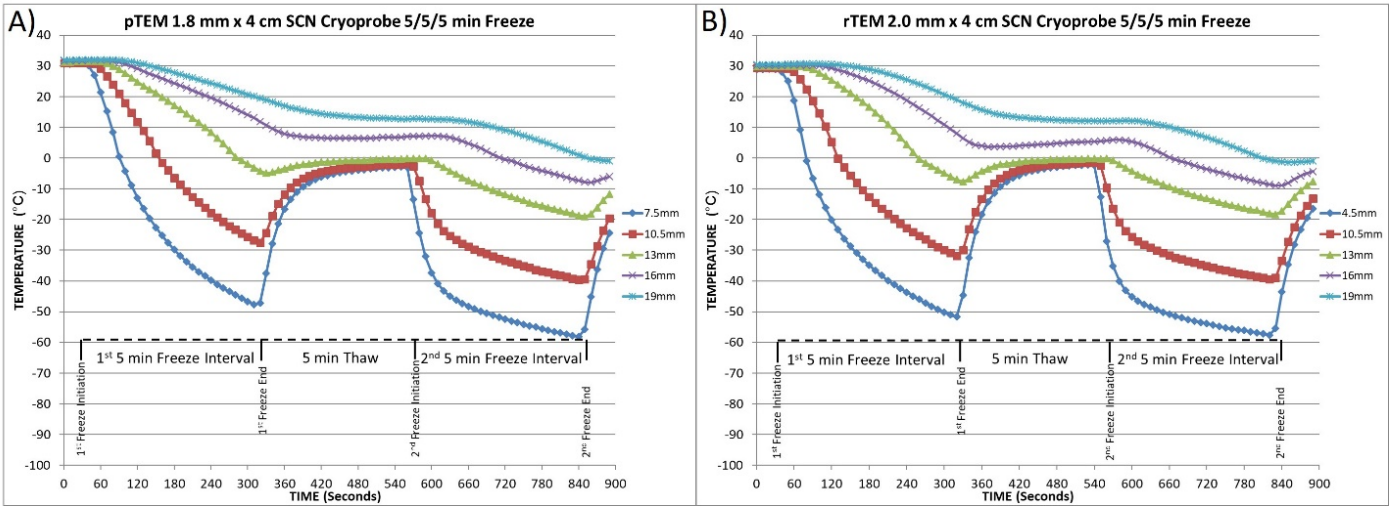

Figure 2. Temperature recording from the center TEM layer during a 5/5/5 freezing protocol

Temperatures were recorded at 10 second intervals at the mid-point of the cryoprobe in the center TEM layer were monitored in A) pTEMs and B) rTEMs at fixed points radiating from the cryoprobe surface during a 5/5/5 freeze/thaw/freeze procedure. Thermal profile assessment revealed a final penetration of the -20°C and -40°C isotherms reaching a diameter of 2.53 cm and 2.02 cm in pTEMs and 2.65 cm and 2.1 cm in rTEMs, respectively, yielding ~45% and ~28% of the frozen mass encompassed within the -20°C and -40°C isotherms, respectively in both pTEMs and rTEMs

Table 2. Analysis of critical isotherm penetration, volume and percent of frozen mass contained within the isotherm following a 5/5/5 freeze with the SCN cryoprobe in the TEM model

	Average Lethal Isotherm Diameter (cm)				Volume (cm)		% of Iceball	
	1st Freeze		2nd Freeze		2nd Freeze		2nd Freeze	
	-20°C	-40°C	-20°C	-40°C	-20°C	-40°C	-20°C	-40°C
pTEM (1.8mm)	2.18 (±0.1)	1.75 (±0.05)	2.53 (±0.11)	2.02 (±0.08)	13.41	8.55	46.4	29.6
rTEM (2.0rnm)	2.29 (±0.1)	1.80 (±0.05)	2.65 (±0.12)	2.10 (±0.09)	14.71	9.24	44.1	27.7

Image analysis of renal cancer rTEM models following freezing using a 2.0 mm x 4.0 cm SCN cryoprobe and a 5/5/5 freeze protocols was also conducted. Given the published increased sensitivity of renal cancer (compared to prostate cancer) to low temperature exposure [7,40,41], studies were conducted to determine what effect the freeze procedure had on renal cancer cell destruction at the center of the probe freeze zone (2 cm level) following completion of a 5/5/5 protocol (Figure 4). As with pTEM studies, lethal zone analysis was conducted at 1 and 24 hours post freeze. Analysis of renal cancer cell destruction following freezing with the 2.0 mm x 4 cm SCN cryoprobe under the 5/5/5 protocol revealed near complete cell destruction to an average distance of 1.75 cm (±0.2 cm) from the probe surface yielding a 3.5 cm (± 0.4 cm) diameter lethal zone around the cryoprobe at the center of the freeze zone (Figure 4). Correlating the zone of destruction with the isotherm data revealed the transition from cancer cell destruction to survival occurring around the -10°C isotherm 1 hour post-thaw with the SCN system. As a result, a 0.22 cm deep rim of incomplete cell destruction was found to remain around the perimeter of the iceball. Follow up analysis 24 hours post freeze revealed a low level of renal cancer cell recovery within the periphery of the iceball compared to that seen at 1 hour post freeze, yielding a final lethal isotherm within the iceball of -20°C for the rTEM's (Figure 4). The ablative volume generated by the SCN system was 26.29 cm^3 in the rTEM samples which accounts for 78.9% of the total frozen volume (Table 3).

It was noteworthy that when comparing the extent of cell death at 1 hr post-thaw to that observed at 24 hr, in both the pTEMs (Figure 3) and rTEMs (Figure 4), the ablative zone decreased slightly at the 24 hr

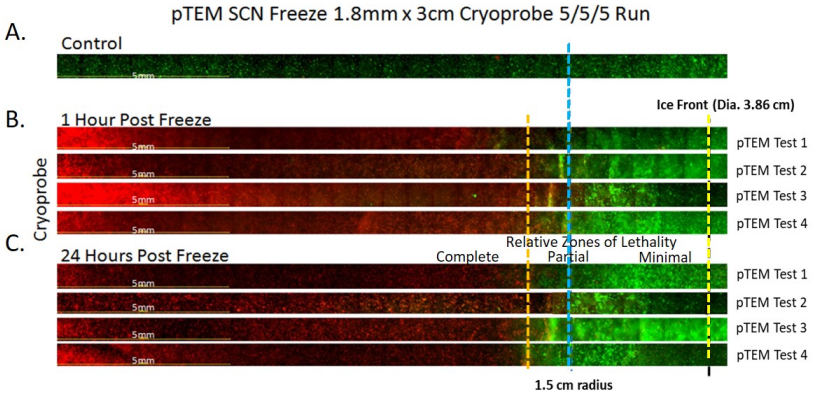

Figure 3. Representative panoramic fluorescent images of prostate cancer TEMs (pTEM) at 1 and 24 hours following freezing

TEMs were frozen under a 5/5/5 min freeze/thaw/freeze protocol using a 1.8 mm SCN Cryoprobe with a 3cm freeze length. Following freezing, TEMs were dissembled and placed into culture for assessment in comparison to controls (A). Following 1 (B) and 24 (C) hours of recovery replicate TEMs from 4 individual freeze tests (Test 1-4) were probed with Calcein-AM (green) and Propidium iodide (red) and visualized using fluorescence microscopy to determine the extent of cell death. Cryoprobe was located at the left of the images. The Blue line marks a 1.5cm radial distance from the probe. The yellow dashed line indicated the edge of the iceball following the 2nd freeze. The orange dashed line represents the approximate location of the -30°C isotherm indicating the transition from partial to complete cell lethality. Analysis of cell death at 24 hours post-freeze revealed average lethal zone equivalent to 60% of the frozen mass

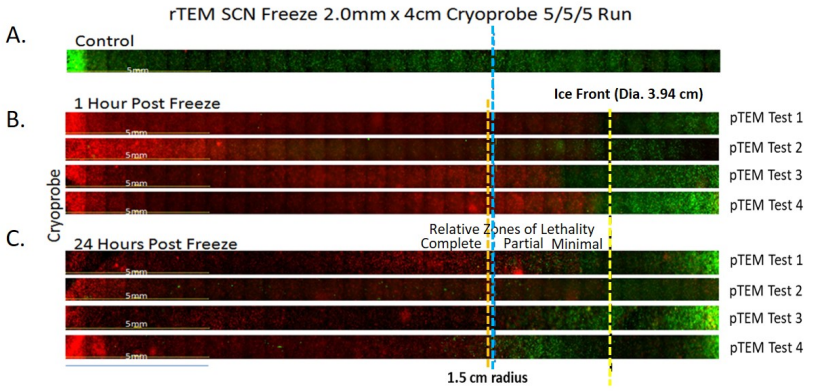

Figure 4. Representative panoramic fluorescent images of renal cancer TEMs (rTEM) at 1 and 24 hours following freezing

TEMs were frozen under a 5/5/5min freeze/thaw/freeze protocol using a 2.0 mm SCN Cryoprobe with a 4cm freeze length. Following freezing, TEMs were dissembled and placed into culture for assessment in comparison to controls (A). Following 1 (B) and 24 (C) hours of recovery replicate TEMs were probed with Calcein-AM (green) and Propidium iodide (red) and visualized using fluorescence microscopy to determine the extent of cell death. Cryoprobe was located at the left of the images. The Blue line marks a 1.5cm radial distance from the probe. The yellow dashed line indicated the edge of the iceball following the 2nd freeze. The orange dashed line represents the approximate location of the -20°C isotherm indicating the transition from partial to complete cell lethality. Analysis of cell death at 24 hours post-freeze revealed average lethal zone equivalent to 78% of the frozen mass

Table 3. Comparison of average Iceball size and zone of cancer cell ablation within the TEM created by the SCN cryoprobe following a 5/5/5 min freeze

	Iceball Size		**Zone of Ablation**		
	Diameter (cm)	Volume (cm)	Diameter (cm)	Volume (cm)	% of Iceball
pTEM (1.8mm)	3.86 (±0.17)	28.87	2.89 (±0.3)	17.43	60.4
rTEM (2.0rnm)	3.94 (±0.19)	33.33	3.54 (±0.4)	26.29	78.9

time point. This was not attributed to cellular regrowth given the short interval between assessment times (23 hr), but instead was likely due to the repair and recovery of cancer cells only experiencing sub-lethal temperatures in the freeze zone periphery. As such, final determination of the ablative zone was based on the 24 hr time point. This observation correlates well with a number of *in vitro* studied which have found the 24 hours time point to more accurately reflect the extent of cryoablative cell death compared to 1 hr post-thaw [26,27,42].

Discussion

Improvements in our understanding of the cellular responses to freezing are now driving a series of technological advancements in cryosurgical devices and clinical techniques. The recognition of the combination of physical and molecular cell death occurring throughout a cryogenic lesion has resulted in the drive to develop advanced technologies designed to deliver colder temperatures more rapidly and within a more defined area to maximize cell death [5]. Today's commercial cryosurgical devices generally fall into one of two categories based on the cryogen employed: compressed gases undergoing Joule-Thomson (JT) cooling or liquid cryogens. For JT devices, the use of pressurized gases establishes rapid cryogen flow and freezing within the cryoprobe freeze zone. Compared to liquid cryogens, however, thermal conductivities are lower, and the nadir temperatures elevated, resulting in a lower rate of heat extraction (e.g. work capacity). Conversely, cryosurgical devices employing liquid cryogens have more efficient heat extraction but are challenged establishing a rapid and steady flow of cryogen to the cryoprobe tip due to liquid boiling and expansion resulting in the formation of a pressure head that slows, or even stops, the flow of cryogen thereby delaying the establishment of freezing temperatures within the freeze zone. In an effort to achieve the rapid freezing of JT devices, yet maintain the heat extraction of liquid devices, we developed a cryosurgical device that employs Supercritical Nitrogen (SCN) as the cryogen [33]. The supercritical state is defined as the phase of matter that exists for a substance beyond its critical point. For nitrogen, this occurs at temperatures below -146.9°C and pressures above 3395.0 kPa (492 psi). In this region of the phase diagram the gaseous and liquid states cannot be distinguished and the nitrogen possesses properties of both phases. In relation to its use as a cryogen, SCN allows for mass flow characteristics similar to nitrogen gas yet retains a thermal conductivity comparable to liquid nitrogen. Previous studies have demonstrated that SCN provides for rapid destruction of cardiac tissue [34,35]. As such, in this study we investigated the potential of the SCN system for targeted ablation of cancerous tissue. To this end, we employed a 3D tissue engineered tumor model (TEM) of prostate and renal cancer to assess the performance of the SCN cryosurgical system. Previous reports have demonstrated that TEMs provide for an effective medium for the assessment of several performance indicators including iceball size, thermal profiling (isotherm distribution) and the resultant lethal zone within the frozen mass following thawing [27,32,37]. With a variety of parameters being investigated in this study, including differing probe diameters, freeze zone length (3 cm and 4 cm) and cancer type (prostate and renal TEMs), extensive characterization and comparative data were generated. While each of the parameters had an impact on an individual group's outcome, several fundamental comparatives emerged from the data.

When comparing the iceball diameter, following a 5/5/5 freeze protocol, the 2.0 mm x 4.0 cm SCN cryoprobe consistently yielded a larger iceball than the 1.8 mm x 3.0 cm SCN cryoprobe. Specifically, it was found that following a 5/5/5 min freeze/thaw/freeze procedure the maximum diameter of the freeze zone attained using the 1.8 mm SCN cryoprobe was 3.86 cm in pTEM samples and using the 2.0 mm SCN cryoprobe 3.94 cm in rTEM samples. This calculate to a frozen TEM tissue volume of 28.87 cm^3 and 33.33 cm^3, respectively (Table 1). This was an anticipated outcome given the ~25% larger surface area (22.5 cm^2 vs 31.4 cm^2).

While the iceball diameter was found to be larger, analysis of the critical isotherms within the frozen mass revealed similar penetration of the -20°C and -40°C isotherm in the pTEM and rTEM following the 5/5/5 protocol. Specifically, within the frozen volume, the -20°C and -40°C isotherms were found to extend to a diameter of 2.53 cm and 2.02 cm, respectively, in pTEMs and 2.65 cm and 2.10 cm in rTEMs. This calculate to a frozen TEM tissue volume for the -20°C and -40°C isotherms of 13.41 cm^3 and 8.55 cm^3 for the 1.8 mm SCN cryoprobe in pTEMs and 14.71 cm^3 and 9.24 cm^3 in rTEMs, respectively. These volumes account for an overall average of 45.3% (-20°C) and 28.7% (-40°C) of the total frozen volume (Table 2).

Comparison of the SCN results to published reports on the thermal performance of an argon JT device with a 2.4 mm diameter x 4.0 cm cryoneedle [39], revealed the SCN Cryosystem with a 2.0 mm x 4.0 cm SCN cryoprobe was able to generate a comparable freeze zone in half the time (5/5/5 vs. 10/5/10). The reported size of the -20°C, and -40°C isotherms generated by the JT system in a phantom gel model were 2.81 cm and 2.11 cm, respectively[3]. These sizes were similar to those generated by the SCN Cryosystem despite the use of a smaller diameter SCN cryoprobe and the freeze medium employed in the JT cryodevice studies was not heat loaded (versus active heating in the current study). Interestingly, when examining total frozen mass, the SCN system was found to generate a colder iceball compared to that reported for argon JT device based on the percentage of the total frozen volume at, or below, the critical isotherms of -20°C (45.3% vs. 40.2%, a 13% increase) and -40°C (28.7% vs. 20.1%, a 43% increase).

The improved performance of the SCN system was even more evident when comparing these findings to reports of the freeze zone generated by an argon JT device using the TEM model [27,32]. In that study, the reported diameter and volume of the total freeze zone created by a 2.4 mm x 4.0 cm JT cryoprobe in a rTEM following a 10/5/10 freeze protocol was 4.63 cm and 38.76 cm^3, respectively [27]. The diameter of the -20°C and -40°C isotherms were reported to be 2.60 cm (12.88 cm^3) and 1.80 cm (6.27 cm^3) thereby comprising 31.9% and 15.3% of the total frozen volume, respectively. With equivalent heat loads, the percent volume of TEM tissue at or below -20°C was 12.2% larger with the SCN system (a 38% increase) and 12.6% larger for TEM tissue at or below -40°C (an 82% increase). The increased distribution of the critical isotherms under physiological heat loads, suggested the generation of a colder, more lethal freeze zone resulting in the volume of complete cell ablation extending further into the periphery of the frozen tissue mass with the SCN Cryosystem.

The increased lethality of the freeze zone generated with the SCN system was further corroborated by live/dead fluorescent imaging of the TEM layers which enabled assessment of the extent of cell death and survival within the frozen region. Based on the transition from live to dead cells within the TEMs, the critical isotherm in the prostate cancer TEMs was found to be ~-30°C and for the renal cancer TEMs ~-20°C. This correlated well with previous *in vitro* and *in vivo* reports which have reported the critical isotherm for prostate cancer to be between -30°C and -40°C and -20°C and -25°C for renal cancer [3,7,19,20,31,41]. In pTEM samples, the total ablative volume at 24 hr post-thaw was found

to be 18.85 cm^3, which equated to 60.4% of the total frozen volume. The rTEM samples, containing renal cancer cells which are more sensitive to freeze insults [7,41], had an ablative volume of 25.65 cm^3 which equaled 78.9% of the total frozen volume (Table 3).

Examining the ablative dose delivered in the TEMs by the SCN system, the data suggested an increase in the percent total ablative volumes of 21.3% and 41.8% for pTEMS and rTEMs, respectively compared to those reported for the argon JT device [27,32]. This increase in ablative volume (54% and 113% increase, pTEM and rTEM, respectively) resulted in a smaller region of incomplete cell death in the freeze zone periphery. Specifically, freeze procedures using the argon JT cryosystem results in a reported 0.80 cm (pTEM) and 0.92 cm (rTEM) deep ring of incomplete cell death at the periphery of the iceball [27], whereas the SCN device yielded a 0.43 cm (pTEM) and 0.22 cm (rTEM) ring. Clinically speaking, with a thinner rim of incomplete cell death the need for a positive freeze margin, and risk of incomplete cancer destruction within the targeted tissue, could be substantially reduced. Further, the risk of collateral damage to non-targeted tissue could also be reduced. For instance, decreasing the positive freeze margin from ~1 cm to ~0.5 cm would result in >40% reduction in non-targeted tissue damage at the periphery of the freeze zone, a volume that could significantly decrease the risk of postoperative complications.

The data presented in this study support the conclusion that the SCN Cryosystem is capable of rapidly creating a ultracold iceball characterized by the deeper penetration of the critical isotherms into a target tissue, thus limiting the ring of incomplete or partial cell death in the periphery of the freeze zone. By combining the thermal performance assessments of phantom gel models and the post-thaw cellular response assessments of *in vitro* cultures, the TEM model provides an effective and versatile platform for the testing, evaluation, and improvement of cryosurgical devices, cryoprobes, and cryoablative techniques. While more reflective of *in vivo* heat load, the TEM model has limitations, given that it does not incorporate/ account for any immunological, wound healing or long term ischemic injury damage which occurs *in vivo* following freezing. To this end, based on its nature and tissue culture environment the TEM model represents a near ideal environment for sample recovery as it provides for optimal oxygen and nutrient delivery throughout the sample. As such, when translating/ comparing these results to *in vivo* scenarios, as with data from all *ex vivo* and phantom models, caution should be taken.

Conclusions

With the recent success and growth of cryoablation there is now a movement toward the increased utilization as well as desire for improved procedural outcome. In order to achieve this in an effective, time efficient manner, new cryotechnologies are being developed to facilitate rapid tissue cooling to more effectively ablate tissue[5,32-35]. This study investigated the performance of one such system, the SCN Cryosystem, for targeted cancer ablation using tissue engineered prostate and renal tumor models. We hypothesized that through the use of the SCN device and probes, rapid, effective, minimally invasive ablation of cancerous tissue could be achieved. The data presented herein demonstrated that the SCN Cryosystem provided for the rapid and effective delivery of a cryoablative "thermal dose" (-20°C and -40°C isotherms) deeper into a frozen tissue mass in half the time of that reported for current argon JT cryosystems under physiological loads (37°C). While the results of this study are promising, given their investigational nature the extent of conclusions which can be drawn are limited; however, the data does suggest that this technology holds promise and that continued assessment of the technology *in vivo* is warranted. Overall, this study suggests that SCN Cryosystem may offers promise as a next generation cryoablation device allowing for the rapid and controlled application of ultra-cold temperatures and efficient freezing of targeted tissue.

Acknowledgements

The authors wish to express their appreciation to Mr. Alind Sahay, MS, MBA for his diligent efforts in the execution of these studies.

Funding

This study was supported in part by funding from the National Institutes of Health and CPSI Biotech and Endocare, Inc.

Conflicts of interests

JMB, AR, KLS, KKS and RVB are employees of CPSI Biotech. JGB has no competing interests.

Authors' contributions

JMB, AR, KLS and KKS performed all experimental design, experimentation and data analysis for this study. RVB and JGB conducted data and experimental design review and assisted in data interpretation. JMB prepared the draft manuscript. JMB, AR, KLS, KKS, RVB and JGB provided review and revision input for the manuscript. All authors read and approved the final manuscript.

Availability of data and material

The data that support the findings of this study are available from CPSI Biotech but restrictions apply to the availability of these data, which were used under license for the current study, and so are not publicly available. Data are however available from the authors upon.

References

1. Gage AA, J Baust (1998) Mechanisms of tissue injury in cryosurgery. *Cryobiology* 37: 171-86. [Crossref]
2. Baust JG (2014) Mechanisms of cryoablation: clinical consequences on malignant tumors. *Cryobiology* 68: 1-11.
3. Hoffmann NE, Bischof JC (2002) The cryobiology of cryosurgical injury. *Urology* 60: 40-49. [Crossref]
4. Baust JG (2009) The pathophysiology of thermoablation: optimizing cryoablation. *Curr Opin Urol* 19: 127-32.
5. Baust JM, Robilotto AT, Gage AA, Baust JG (2016) Enhanced Cryoablative Methodologies. In: Eds: Bishof J, Xi Y. Multiscale Technologies for Cryomedicine. WSPC Publishers p, 3-24.
6. Baust JG, Gage AA (2005) The molecular basis of cryosurgery. *BJU Int* 95: 1187-1191. [Crossref]
7. Clarke DM (2007) Cryoablation of renal cancer: variables involved in freezing-induced cell death. *Technol Cancer Res Treat* 6: 69-79.
8. Klossner DP (2008) Cryoablative response of prostate cancer cells is influenced by androgen receptor expression. *BJU Int* 101: 1310-1316. [Crossref]
9. Baust JG (2010) Integrin involvement in freeze resistance of androgen-insensitive prostate cancer. *Prostate Cancer Prostatic Dis* 13: 151-61.
10. Han B, Swanlund DJ, Bischof JC (2007) Cryoinjury of MCF-7 human breast cancer cells and inhibition of post-thaw recovery using TNF-alpha. *Technol Cancer Res Treat* 6: 625-34.
11. Cohen JK (2008) Ten-year biochemical disease control for patients with prostate cancer treated with cryosurgery as primary therapy. *Urology* 71: 515-8. [Crossref]
12. Long JP (2001) Five-year retrospective, multi-institutional pooled analysis of cancer-related outcomes after cryosurgical ablation of the prostate. *Urology* 57: 518-23.
13. Bahn DK (2002) Targeted cryoablation of the prostate: 7-year outcomes in the primary treatment of prostate cancer. *Urology* 60: 3-11.

14. Bahn D (2012) Focal cryotherapy for clinically unilateral, low-intermediate risk prostate cancer in 73 men with a median follow-up of 3.7 years. *Eur Urol* 62: 55-63. [Crossref]

15. Spiess PE, Given RW, Jones JS (2012) Achieving the 'bifecta' using salvage cryotherapy for locally recurrent prostate cancer: analysis of the Cryo On-Line Data (COLD) registry data. *BJU Int* 110: 217-20.

16. Spiess PE (2013) Outcomes of salvage prostate cryotherapy stratified by pre-treatment PSA: update from the COLD registry. *World J Urol* 31: 1321-1325.

17. Cheetham P (2010) Long-term cancer-specific and overall survival for men followed more than 10 years after primary and salvage cryoablation of the prostate. *J Endourol* 24: 1123-1129. [Crossref]

18. Babaian RJ (2008) Best practice statement on cryosurgery for the treatment of localized prostate cancer. *J Urol* 180: 1993-2004.

19. Baust JG (2007) Issues critical to the successful application of cryosurgical ablation of the prostate. *Technol Cancer Res Treat* 6: 97-109.

20. Klossner DP (2007) Cryosurgical technique: assessment of the fundamental variables using human prostate cancer model systems. *Cryobiology* 55: 189-99.

21. Caso JR (2012) Complications and postoperative events after cryosurgery for prostate cancer. *BJU Int* 109: 840-845. [Crossref]

22. Onik G (1991) Percutaneous transperineal prostate cryosurgery using transrectal ultrasound guidance: animal model. *Urology* 37: 277-281.

23. Thompson I, Thrasher JB, Aus G, Burnett AL, Canby-Hagino ED, et al. (2007) Guideline for the management of clinically localized prostate cancer: 2007 update. *J Urol* 177: 2106-2131. [Crossref]

24. Baust JG (2015) Re-purposing cryoablation: a combinatorial 'therapy' for the destruction of tissue. *Prostate Cancer Prostatic Dis* 18: 87-95.

25. Gage AA, Baust JG (2007) Cryosurgery for tumors. *J Am Coll Surg* 205: 342-356. [Crossref]

26. Hollister WR, Mathew AJ, Baust JG (1998) The effects of freezing on cell viability and mechanisms of cell death in an in vitro human prostate cancer cell line. *Mol Urol* 2: 13-18.

27. Baust JM, Robilotto AT, Snyder KK, Santucci KL (2017) Assessment of cryosurgical device performance using an in vivo-like 3-D tissue engineered cancer model. *Tech Cancer Res Treat* 16: 900-909.

28. Clarke DM (2004) Addition of anticancer agents enhances freezing-induced prostate cancer cell death: implications of mitochondrial involvement. *Cryobiology* 49: 45-61. [Crossref]

29. Han B, Iftekhar A, Bischof JC (2004) Improved cryosurgery by use of thermophysical and inflammatory adjuvants. *Technol Cancer Res Treat* 3: 103-11.

30. Clarke DM (2007) Targeted induction of apoptosis via TRAIL and cryoablation: a novel strategy for the treatment of prostate cancer. *Prostate Cancer Prostatic Dis* 10: 175-184.

31. Baust JM, Rabin Y, Polascik T, Robilitto AT, Snyder KK, et al. (2018) Defeating cancers adaptive defensive-strategies using thermal ablative therapies. *Technology in Cancer Research & Treatment* 17: 1-16. [Crossref]

32. Baust JM (2014) Assessment of SCN and argon cryoablation devices in an in vivo like 3-D tissue engineered prostate and renal cancer model. Poster session presented at: in ACCryo 2014-Advances in Thermal Abaltive Therapy and Biopreservation, Annual Meeting of the American College of Cryosurgery. Key Largo, FL.

33. Robilotto AT, Snyder KK, Baust JM, Baust JG, Cheeks R (2014) Cryogenic system and method of use, USPTO patent 8,784,409, EndoCare, Inc.

34. Baust JM, Robilotto AT, Guerra P, Dubuc M (2018) Assessment of a novel cryoablation device for the endovascular treatment of cardiac tachyarrhythmia's. *Sage Open Medicine* 6: 1-13. [Crossref]

35. Baust JM, Robilotto AT, Snyder KK, Van Buskirk RG, Baust JG (2017) Development of a novel epicardial cryoablation system for the treatment of cardiac tachyarrhythmias. *Trends in Medicine* 18: 1-10.

36. Robilotto AT (2007) Development of a tissue engineered human prostate tumor equivalent for use in the evaluation of cryoablative techniques. *Technol Cancer Res Treat* 6: 81-89.

37. Robilotto AT (2013) Temperature-dependent activation of differential apoptotic pathways during cryoablation in a human prostate cancer model. *Prostate Cancer Prostatic Dis* 16: 41-49.

38. Baust JG, Santucci KL, Snyder KK, Robilotto AT, Van Buskirk RG, et al. (2015) Tissue engineered model and method of use, USPTO patent 9,213,025, CPSI Holdings LLC.

39. Healthtronics V probe, 2011, 5 position variable cryoprobe. [pdf] Austin, TX: Available at https://www.healthtronics.com/sites/default/files/resources/V-probe-Instrument-Sheet.pdf.:

40. Aron M, Kamoi K, Remer E, Berger A, Desai M, et al. (2010) Laparoscopic renal cryoablation: 8-year, single surgeon outcomes. *J Urol* 183: 889-895. [Crossref]

41. Gage AA, Baust JM, Baust JG (2009) Experimental cryosurgery investigations in vivo. *Cryobiology* 59: 229-243.

42. Robilitto AT, Baust JM, Van Buskirk RG, Gage AA, Baust JG (2010) Differential cell signaling in human prostate cancer cells frozen in monolayers versus a three dimensional prostate tumor model: The PI3 kinase-AKT pathway. *Cryobiology* 61: 364.